# *Authentication of Iceland Moss (Cetraria islandica) by UPLC-QToF-MS chemical profiling and DNA barcoding*

**Authentication of Iceland Moss by UPLC-QToF-MS chemical profiling and DNA barcoding**

Maonian Xu[a], Starri Heidmarsson[b], Margret Thorsteinsdottir[a], Marco Kreuzer[c], Julie Hawkins[c], Sesselja Omarsdottir [a], Elin Soffia Olafsdottir[a,*]

[a] Faculty of Pharmaceutical Sciences, University of Iceland, Hagi, Hofsvallagata 53, IS-107 Reykjavik, Iceland (Emails: xum1@hi.is, margreth@hi.is, sesselo@hi.is, elinsol@hi.is)

[b] Icelandic Institute of Natural History, Akureyri Division, IS-600 Akureyri, Iceland (Email: starri@ni.is)

[c] School of Biological Sciences, University of Reading, Reading RG6 6BX, United Kingdom (Emails: marcokrz@gmail.com, j.a.hawkins@reading.ac.uk)

* Corresponding author

Elin Soffia Olafsdottir, Ph.D, Professor

Faculty of Pharmaceutical Sciences

University of Iceland

Hagi, Hofsvallagata 53,

IS-107 Reykjavik, Iceland

Tel: +354 5255804

Fax: +354 5254071

Email: elinsol@hi.is

**Abstract**

The lichen *Cetraria islandica* or Iceland Moss is commonly consumed as tea, food ingredients (e.g. in soup or bread) and herbal medicines. *C. islandica*, which has two chemotypes, can be difficult to distinguish from the sister species *Cetraria ericetorum*. They are collectively referred to as the *Cetraria islandica* species complex. This study aimed to use an UPLC-QToF-MS chemical profiling together with DNA barcoding to distinguish species and chemotypes of the *C. islandica* species complex. Our results show that the two chemotypes of *C. islandica* are clearly distinguishable from each other and from *C. ericetorum* by the chemometric approach. The RPB2 barcode was able to differentiate *C. islandica* from *C. ericetorum* with a barcode gap, but the widely used nrITS barcode failed. Neither of them could discriminate chemotypes of *C. islandica*. In conclusion, this integrative approach involving chemical profiling and DNA barcoding could be applied for authentication of Iceland Moss materials.

Keywords: *Cetraria islandica*, *Cetraria ericetorum*, DNA barcoding, chemical profiling, authentication

## 1. Introduction

Taxonomically, *Cetraria islandica* or Iceland Moss is not a moss species but a lichen taxon and the classification is based on the symbiotic fungal partner (Parmeliaceae, ascomycete) (Ingolfsdóttir, 2000). This lichen is consumed in Iceland as tea, food ingredients (e.g. in milk soups and bread) and herbal medicines (Xu et al., 2016). Considerable morphological and chemical variations have been found among Icelandic populations of *C. islandica* and two chemotypes have been reported (Kristinsson, 1969). They consist of the fumarprotocetraric acid (FA)-producing and FA-deficient races, where the latter chemotype has exclusively been found in Iceland (Kristinsson, 1969). Traditional use seems to favor the FA-deficient chemotype of *C. islandica*, which is believed to be less bitter (Kristinsson, 1968). Furthermore, the species boundaries between *C. islandica* and its sibling species *Cetraria ericetorum* are still ambiguous: *C. ericetorum* has similar morphology to certain morphotypes of *C. islandica* and it is reported to be FA-deficient. Together *C. islandica* and *C. ericetorum* are collectively called the *Cetraria islandica* species complex (Kristinsson, 1969; Thell, Stenroos, & Myllys, 2000). Their chemical profiles, particularly of the *C. islandica* FA-deficient chemotype and *C. ericetorum*, have not been thoroughly investigated for food safety, and an accurate identification method for these lichen materials is needed.

Chemical profiling or fingerprinting, in particular when using an untargeted approach, can directly detect chemical hazards and contaminants in food or herbal materials, with the limitation that their species sources cannot be determined (de Boer, Ichim, & Newmaster, 2015). Chemometric analysis using complex metabolite datasets has shown great potential in the inspection of food adulteration as well as in the characterization of markers for adulteration detection (Cubero-Leon, Peñalver, & Maquet, 2014).

Untargeted chemical profiling is especially useful in the distinction of closely-related plant species, where certain genetic markers may not be informative (Messina, Callahan, Walsh, Hoebee, & Green, 2014). That approach has been successfully applied to the lichen *Ramalina siliquosa* complex using liquid chromatography-mass spectrometry (LC-MS) (Parrot, Jan, Baert, Guyot, & Tomasi, 2013).

Recently, DNA barcoding has emerged as an effective tool in the identification of plant and animal materials using defined species-specific DNA markers. It has found wide application in the authentication and traceability of food materials (Galimberti et al., 2013). This approach has been extended to the authentication of multiple ingredients samples using a more advanced DNA metabarcoding approach, which involves next generation sequencing (Staats et al., 2016). Practically, DNA barcoding has been applied for authentication of fungi-based dietary products (Raja, Baker, Little, & Oberlies, 2017). Furthermore, identification of lichenized fungi using DNA barcoding has been successfully performed using the fungal nuclear ribosomal internal transcribed spacer region (nrITS) (Kelly et al., 2011), which has been proposed as the universal DNA barcode for fungi (Schoch et al., 2012).

Two DNA barcodes, nrITS and RPB2 (the second largest subunit of ribosomal polymerase II) were selected for this study on the *C. islandica* lichen materials. Although the widely used nrITS region is known to provide a sufficient amount of variation to distinguish between most fungal species and is represented by many reference sequences in public databases, some drawbacks for DNA barcoding and especially DNA metabarcoding have been reported (Větrovský, Kolařík, Žifčáková, Zelenka, & Baldrian, 2016). While nrITS can identify species, its multi-copy nature of the ITS region may render problems with relative quantification of species in mixed

samples. In other cases, intra-individual polymorphism including multiple functional genes, putative pseudo genes or recombinants hamper identifications (Mark, Cornejo, Keller, & Flück, 2016). The single-copy RPB2 gene has been proposed as an alternative to the nrITS region, which could overcome some of these challenges (Větrovský et al., 2016). The performance of RPB2 will be compared to that of nrITS in our study.

The overall aim of this study was to explore the usefulness of an authentication approach for *Cetraria islandica* species complex using UPLC-QToF-MS chemical profiling and DNA barcoding. Specific objectives were: Firstly, to distinguish chemotypes of the species complex by comparing their UPLC-QToF-MS chemical profiles using chemometric data analysis, and secondly to compare the discriminatory power of RPB2 and nrITS barcodes for the taxa of the *C. islandica* species complex.

## 2. Materials and Methods

### 2.1 Sampling and chemotype identification

*Cetraria islandica* (L.) Ach. (English: Iceland Moss; Icelandic: fjallagrös) and *Cetraria ericetorum* Opiz specimens were collected in Iceland. Authentic specimens of *C. islandica* are provide by lichenologists from the Icelandic Institute of Natural History, Akureyri, Iceland (AMNH). Collected voucher specimens are deposited at the AMNH herbarium. Intraspecific morphological variation of Iceland Moss (*C. islandica*) as well as the interspecific similarity between the two species (*C. islandica* and *C. ericetorum*) can be seen in Figure 1. Additional *C. ericetorum* type specimens were kindly provided by Dr. Stefan Ekman, Museum of Evolution, Uppsala University, Uppsala, Sweden. The chemotypes of *C. islandica* and *C. ericetorum* were tested using a conventional spot testing

method (Kristinsson, 1969). Briefly, a small fragment was cut from a thallus with a blade, and drops of *p*-phenylendiamine (PD) solution (ca. 2% in ethanol) were added to lichen medulla on a white paper with a glass capillary tube. Then the medullary color reactions were visualized under a stereoscope. Specimens showing a red medullary color after spot testing were assigned as PD+, while the ones without color change as PD-. PD spot testing was carried out on fragments from three different parts of the thallus, to make sure the chemotype. Fragments were discarded immediately after testing. Voucher information and gene accession numbers are provided in Online Resource (see Table S1). In total, 30 specimens of PD+ *C. islandica*, 15 specimens of PD- *C. islandica* and 18 specimens of uniformly PD- *C. ericetorum* were identified.

### 2.2 Chemical profiling

#### 2.2.1 LC-MS analysis

Air-dried lichen thallus (ca. 20 mg) was weighed and ground into powders under liquid nitrogen. Powdered lichen materials were macerated with acetone under shaking in ambient temperature for 2 h. The extraction was repeated twice. Extracts were combined and evaporated with nitrogen gas flow. Dried residues were then solubilized in HPLC-grade acetonitrile (ACN), diluted into 0.1 mg/mL and filtered (pore size 0.45 μm; GE healthcare, UK) before analyses by Waters ACUITY UPLC™ (Waters Corporation, Milford, MA, USA) coupled to Waters Q-ToF SYNAPT G1 mass spectrometer (Waters MS Technologies, Manchester, UK).

The UPLC system was equipped with a binary solvent delivery system and autosampler. Chromatographic separation of lichen compounds was conducted on an ACQUITY UPLC BEH C18 column (2.1 mm x 100 mm,

1.7 μm; Waters corp., Milford, MA, USA). The column oven was kept at 40ºC and the autosampler was maintained at 6.0ºC. The mobile phase consisted of solvent A: $H_2O$ with 0.1% formic acid in water and solvent B: 0.1% formic acid in ACN. Gradient elution was used at a flow rate of 0.40 mL/min as follows: 30% B, 0-1 min; linear gradient from 30% B/70% A to 70% B/30% A, 1-3 min; linear gradient from 70% B/30% A to 100% B, 3-9 min; holding at 100% B, 9-13 min; linear gradient from 100% B to 30% B/70% A, 13-14 min; holding at 30% B/70% A, 14-15 min. Pooled samples were used as quality control. The injection volume was 5 μL.

The Synapt G1 QToF-MS mass spectrometer was operated in negative electrospray ionization mode (capillary voltage 3.0 kV, source temperature 120ºC, desolvation temperature 400ºC, cone gas flow 50 L/h, desolvation nitrogen gas flow 800 L/h). Ions with mass range 50 to 1600 m/z (mass to charge ratio) were scanned. All samples were analyzed in triplicates. Details of UPLC-QToF-MS analysis are as previously described (Xu et al., 2017). The UPLC-QToF-MS system and data acquisition were controlled by the MassLynx v4.1 software (Waters Corp., Milford. USA).

#### 2.2.2 Chemometric data analysis

MS spectra were aligned and normalized using MakerLynx v4.1. Collection parameters were set as 50 counts, mass window 0.05 Da and retention time window 0.2 min. Replicate percentage value was set at 50%. Normalized data were introduced into SIMCA v14.1 software (Sartorius Stedim Data Analytics, Umeå, Sweden) for principal component analysis (PCA). PCA could provide a holistic overview of the grouping of lichen specimens, which was based on chemical data from organic extracts. Compounds were identified by comparing their MS/MS spectra and fragmentation patterns

with those from isolated pure compounds, previously published data and public databases (Metlin and ChemSpider).

### 2.3 Molecular analysis

#### 2.3.1 DNA extraction, PCR and sequencing

Air-dried lichen residues after acetone maceration were used for total DNA extraction following the CTAB protocol (Cubero, Crespo, Fatehi, & Bridge, 1999). Lichen DNA extracts were stored in TE buffer (pH 8.0) at -20ºC until use. Polymerase chain reactions (PCRs) were performed to amplify the fungal nuclear ribosomal internal transcribed spacer (nr ITS) and the second largest subunit of RNA polymerase II (RPB2). Each reaction (25 μL) contained 1×standard Taq reaction buffer, 200 μM dNTPs, 0.2 μM forward and reverse primer, 1.25 units of Taq DNA polymerase (New England Biolabs), 1 μL DNA template, and PCR-grade water. The fungi-specific primers used for the amplification of nr ITS region were: ITS1F (5'-CTTGGTCATTTAGAGGAAGTAA-3') (Gardes & Bruns, 1993) and ITS4 (5'-TCC CCGCTTATTGATATGC-3') (White, Bruns, Lee, & Taylor, 1990), while the primers for the RPB2 regions were: RPB2-6F (5'-TGGGGKWTGGTYTGYCCTGC-3') (Liu, Whelen, & Hall, 1999) and fRPB2-7cR (5'-CCCATRGCTTGYTTRCCCAT-3') (Liu et al., 1999). PCR amplification was carried out in a Perkin-Elmer Gene Amp PCR system 9700 thermal cycler. The PCR cycling conditions for nrITS were: initial denaturation at 94ºC for 3 min, 34 cycles of 94ºC for 40 s, 54ºC for 40 s, 68ºC for 1 min, then final extension at 68ºC for 5 min before cooling down to 4ºC. A touchdown PCR program was used for RPB2 region: 94ºC for 4 min, followed by 6 cycles of 94ºC for 1min, 55-50ºC (decrease 1ºC per cycle) for 1min and 68ºC for 1min, then 32 cycles of 94ºC for 1min, 50ºC for 1min and 68ºC for 1min, and final extension at 68ºC for 7min, before

cooling down at 4ºC. Amplicons were visualized in 1.3% agarose gel (gel picture refers to Online Resource Figure S1), purified using ExoSAP (Fermentas) and sent for Sanger sequencing by Marogen Inc. using the same set of primers as used in PCRs.

### 2.3.2 DNA barcoding analysis

The discriminatory power of the nrITS and RPB2 barcodes was assessed according to the monophyly criterion and the DNA barcoding gap concept (Meyer & Paulay, 2005). The sequences representing each barcode were aligned using MAFFT v7.215 (Katoh & Standley, 2013) with default parameters and trimmed if necessary. Phylogenetic trees using the Genbank sequences of *C. sepincola* (accession number KC990137.1 for nrITS) as outgroups were built with RAxML v. 8.0.26 (Stamatakis, 2014) with 100 rapid bootstrap replicates under the GTRGAMMA model. The DNA barcode gap analysis was conducted on *C. islandica* and its sister species *C. ericetorum* using the R package SPIDER (Brown et al., 2012), using the best-fitting substituion models to measure pair-wise distances. Best-fitting substitution models for each region (TIM2+G for nrITS; TIM2+I for RPB2) were chosen by using the Aikaike Information Criterion (AIC) in jModelTest 2 (Darriba, Taboada, Doallo, & Posada, 2012). Because the TIM2+G and TIM2+I models were not available in the R package APE (Paradis, Claude, & Strimmer, 2004), which was used to calculate pairwise distances, the next best-fitting model for both alignments, TrN+G, was used.

The number of false positive and false negative identifications along a DNA divergence threshold were calculated and plotted using the R package SPIDER (Brown et al., 2012). Additionally, the minimum interspecific and maximum intraspecific divergence for each sequence was calculated and plotted.

## 3. Results and Discussion

### 3.1 Chemical profiling and chemometric data analysis

Chemical profiling of *C. islandica* organic extracts has been carried out before using high performance liquid chromatography-ultraviolet detection (HPLC-UV) (Fernández-Moriano, Divakar, Crespo, & Gómez-Serranillos, 2015; Gudjónsdóttir & Ingólfsdóttir, 1997). Those previously used methods lack separation efficiency and sensitivity, and thus may underestimate the chemical diversity of *C. islandica*, e.g. (+)-roccellaric acid **6** was found in *C. islandica* using a fluorous tag-catch and release approach (Horhant, Lamer, Boustie, Uriac, & Gouault, 2007), but was previously overlooked due to poor chromatographic separation. Additionally, HPLC-UV (Fernández-Moriano et al., 2015) analysis using high UV wavelengths may overlook the content of those aliphatic lichen acids (i.e. compounds **5**-**8**), which are poor UV absorbants. The current UPLC method achieved the separation of compound **6** from its analogues **7** and **8**. A list of detected compounds is provided in Table S2, and the structures of major lichen secondary metabolites from the *C. islandica* species complex are illustrated in Figure 2.

Compounds **1**-**8** were identified in our study by comparing their molecular masses, fragmentation pathway and chromatographic properties with reference data as well as authentic standards isolated in previous studies (Bessadóttir et al., 2014; Gudjónsdóttir & Ingólfsdóttir, 1997). $MS^2$ spectra of each compound and their fragmentation patterns are provided in Online Resource (see Figures S2-S4). MS chromatograms (Figure 3) show that (+)-protolichesterinic acid **7** and its derivatives (i.e. **6** and **8**) are the dominant compounds in organic extracts detected in negative ion mode, followed by minor components, such as protocetraric acid **1** and fumarprotocetraric acid

**3**. The stereochemical diversity of (+)-protolichesterinic acid **7** seems to be largely underestimated before, since two compounds (i.e. **7A** and **7B**) were detected with the same molecular formula, molecular ions and fragmentation patterns (Figure S4) with compound **7** (Table S2 and Figure 3). In *C. ericetorum*, an additional unknown compound **6A** in the peak eluting out at 5.77 min (Figure 3c) was detected having the same mass to charge ratio as well as fragmentation pattern as (+)-roccellaric acid **6**, which suggests that **6A** could be a stereoisomer of compound **6** (Figure S4). Up to now, only one stereochemical form of roccellaric acid has been reported in nature, namely (+)-roccellaric acid **6** in *C.islandica* (Horhant et al., 2007). Three additional stereochemical forms have been synthesized by Mulzer et al. (Mulzer, Salimi, & Hartl, 1993). Minor compounds **1** and **3** eluted quite early ($t_R$ = 2.49 and 2.96 min, respectively) under the chromatographic conditions used, reflecting that they are more water-soluble than compounds **5**-**8**. Fumarprotocetraric acid **3** (50 mg) is reported to be moderately soluble in 30 mL phosphate buffer at pH 7.4 (Syers, 1969), while the solubility of compound **3** is low (1 mg/L) in 90% acetonitrile with 1% phosphoric acid (Gudjónsdóttir & Ingólfsdóttir, 1997). Thus, polarity and pH of the extraction solvent can be expected to have considerable influence on the extraction efficiency of these lichen acids (i.e. compounds **1**-**4**).

As a conventional diagnostic tool, the PD spot test was used to check the chemotype and the presence of compound **3** in *C. islandica* (Kristinsson, 1969). From LC-MS chromatograms shown in Figure 3, the red color reaction by PD spot testing was found to correlate with the presence of compouds **1** and **3**, while these compounds were absent in the PD- *C. islandica* chemotype and *C. ericetorum*. The presence of the aliphatic lichen acids (i.e. compounds **5**-**8**) did not result in a red color reaction. The co-occurence of compouds **1** and **3** in organic extracts of *C. islandica* has been found in literature (Fernández-Moriano et al., 2015).

The two-component PCA score plot (Figure 4) of the UPLC-QToF-MS data provides the visualization of how different chemical groups relate to each other. Three chemical groups were formed based on their chemical profiles, representing the PD- (CI PD-) and PD+ chemotypes (CI PD+) of *C. islandica* and *C. ericetorum* (CE). The first component explains 43.6% chemical variations, mainly interspecific differences between CE and CI. The secondary component accounts for 10.4% variations, mainly intraspecific differences between CI PD+ and CI PD-. PCA is a useful tool in summarizing metabolite data and revealing groupings of food ingredients from different biological origins (Azilawati, Hashim, Jamilah, & Amin, 2015; Cubero-Leon et al., 2014). From the Figure 4, the lichen *C. islandica* shows high intraspecific chemical variations in Iceland with two chemotypes recognized as reported before (Kristinsson, 1969), while Icelandic *C. ericetorum* shows relatively less variation, even when compared with non-Icelandic *C. ericetorum* specimens. This could partly be explained by the limited distribution of CE, resulting in less variation. CE has a restricted geographic distribution in north and east Iceland, whereas CI has a rather wide distribution around Iceland (Thell & Moberg, 2011).

### 3.2 DNA barcoding

Sizes of PCR products were ca. ~600-900 bp for fungal nrITS and ca. ~900 bp for fungal RPB2 (Online Resource Figure S1). The variation of the fungal nrITS PCR products was due to the presence of a group I intron sequence in the longer amplicons, and absence in the short ones. In total 97 new sequence were obtained, including 48 for RPB2 and 49 for fungal nrITS. PCRs of a few old herbarium reference specimens were not successful (Online Resource Table S1).

The phylogenetic tree based on the ITS region (Figure 5a) shows that *C. ericetorum* is paraphyletic and nested within the *C. islandica* clade, whereas both *C. ericetorum* and *C. islandica* are monophyletic in the RPB2 tree (Figure 5b). Therefore the phylogenetic analyses support RPB2 as a barcode with power to discriminate between the two species of *Cetraria*, but shows that the nrITS barcode does not discriminate the species under study. The pairwise distance analysis supports this interpretation, revealing that RPB2 is able to distinguish the two taxa, whereas the nrITS region always yields false positive or negative identifications (Figure 6). There are other cases where the nrITS region fails to discriminate lichenized fungi (Kelly et al., 2011; Pino-Bodas, Martín, Burgaz, & Lumbsch, 2013), though the nrITS region revealed interspecific barcoding gaps among most species of genera *Melanelia* and *Montanelia* ( Leavitt et al., 2014; Pino-Bodas et al., 2013). The failure of the nrITS region in this case might be attributed to intragenomic polymorphism in the ITS region, a phenomenon described in other lichen-forming fungi (Kelly et al., 2011; Mark et al., 2016). It has also been reported that the nrITS region alone is not suitable to estimate the phylogenetic relationships within the *C. islandica* group (Thell et al., 2000).

The limited application of RPB2 as a barcoding region has been explained by difficult PCR amplification and sequencing (Schoch et al., 2012). Specimens stored for over 3 years have shown problems in PCR amplification (Kelly et al., 2011). We have, however, not encountered a PCR amplification problem for either locus even with specimens which are 15 years old. Successful PCR amplification of the RPB2 region using even older specimens (*Cladonia* sp.) of about 30 years has also been recorded (Pino-Bodas et al., 2013). Age-dependent problems with PCR amplification may be taxon-specific, as well as influenced by the DNA extraction method in use. We noted that the sequence alignment of RPB2 is much simpler. In contrast to the hypervariability of the nrITS region, RPB2 is also

recommended as an alternative marker for phylogenetic analysis (Větrovský et al., 2016). We therefore reject the nrITS region and propose the RPB2 region as an efficient DNA barcode for testing medicinal products containing Iceland Moss, at least in terms of discriminating between *C. ericetorum* and *C. islandica*.

Although the RPB2 region is effective for discriminating between species, chemotypes of *C. islandica* are not discriminated (Figure 5). In Figure 5b, *C. islandica* specimens from Iceland show two strongly supported clades, I and II. All of the *C. islandica* PD- chemotype specimens fall into clade I, but are interspersed with PD+ chemotypes, while clade II contains exclusively PD+ *C. islandica* specimens. Some lichen chemotypes have been shown to be monophyletic (Fehrer, Slavíková-Bayerová, & Orange, 2008), but they can also be not (Lutsak, Fernández-Mendoza, Nadyeina, Şenkardeşler, & Printzen, 2017).

Domestically, *Cetraria islandica* is sold as whole lichen-thalli food ingredients or tea in Iceland. Accurate identification is generally not difficult for taxonomic experts, but it may prove intractable to identify powdered lichen materials, which lack morphological or sometimes chemical characters. DNA barcoding as outlined here could substantially facilitate identification by comparing new sequence data with reference data generated from expertly identified voucher specimens.

The current study focused on the authentication of natural lichen materials without downstream processing. In case of highly processed herbal materials where DNA may undergo considerable degradation, an alternative method could be double gene targeting PCR, which amplifies selected shorter regions (e.g. 70-150 bp) (Hossain et al., 2016, 2017).

### 3.3 The advantage of the integrative approach for authentication of Iceland Moss

Lichen material authentication generally operates at the species level and as shown in this study DNA barcoding using RPB2, is an efficient method for species identification in the *C. islandica* species complex. The advantage of DNA barcoding is in identification of raw plant materials, sources of contaminants and species composition (de Boer et al., 2015), which is beyond the scope of chemical analysis. Generally, chemical profiling of lichen secondary metabolites do not have the independent role in identification/authentication of lichen species (Lumbsch, 1998). First, the utility of metabolite data in lichen identification varies among lichen taxa/populations. Our results (Table S2 and Figure 4) have demonstrated the utility of chemical profiling in discriminating species (*C. islandica* and *C. ericetorum*) and chemotypes (PD+ and PD-) in the *Cetraria islandica* species complex. However, chemical profiling may have limited utility in species discrimination where remarkable chemical variations (e.g. different in major lichen compounds) are present, such as the lichen *Ramalina siliquosa* (Lumbsch, 1998; Parrot et al., 2013). Such a huge variation may pose a challenge in lichen identification: how much chemical variation is allowed to define a species? To address this problem, it has been suggested that chemical characters be correlated with other characters, preferentially genetic sequence data (Lumbsch, 1998). The correlation between phylogenetic relationship and chemotyping (i.e. PD+ and PD-) was investigated in our study (Figure 5b).

Although chemical profiling does not have an independent role in lichen species identification/Iceland Moss authentication, it is indispensable for the quality control of marker or health-beneficial components. It can provide both qualitative and quantitative information on phytochemical composition

during extraction and downstream processing. Coupled to chemometric tools, chemical profiling could also be used in differentiation of intraspecific chemical variants, which is superior to DNA barcoding.

In conclusion, this study highlights the integrative use of chemical profiling and DNA barcoding for the authentication of Iceland Moss. The members of *Cetraria islandica* species complex were easily characterized using chemometric tools. Furthermore, DNA barcodes were compared and the locus RPB2 proved to be superior to nrITS in distinguishing species of *C. islandica* species complex. Our study shows how chemical profiling and DNA barcoding can be used to differentiate chemical variants and species in the complex, and suggests the use of this integrated approach for accurate characterization of this closely related taxa as well as other plant materials used for human consumption.

**Acknowledgements**

This work was supported by the People Programme (Marie Curie Actions) of the European Union's Seventh Framework Programme FP7/2007-2013/ [grant number 606895]; Bergthora and Thorsteinn Scheving Thorsteinsson Fund. Professor Kristinn P. Magnusson and Ph.D student Maney Sveinsdottir, University of Akureyri, Iceland, are acknowledged for their help in molecular analysis. The authors are particularly grateful to Dr. Hörður Kristinsson (AMNH) for specimen collection and thoughtful discussion.

**Conflicts of interest:** none

**References**

Azilawati, M. I., Hashim, D. M., Jamilah, B., & Amin, I. (2015). RP-HPLC method using 6-aminoquinolyl-N-hydroxysuccinimidyl carbamate incorporated with normalization technique in principal component analysis to differentiate the bovine, porcine and fish gelatins. *Food Chemistry*, *172*, 368–376.

Bessadóttir, M., Skúladóttir, E., Gowan, S., Eccles, S., Ómarsdóttir, S., & Ögmundsdóttir, H. M. (2014). Effects of anti-proliferative lichen metabolite, protolichesterinic acid on fatty acid synthase, cell signalling and drug response in breast cancer cells. *Phytomedicine*, *21*(12), 1717–1724. https://doi.org/10.1016/j.phymed.2014.08.006

Brown, S. D. J., Collins, R. A., Boyer, S., Lefort, M. C., Malumbres-Olarte, J., Vink, C. J., & Cruickshank, R. H. (2012). Spider: An R package for the analysis of species identity and evolution, with particular reference to DNA barcoding. *Molecular Ecology Resources*, *12*(3), 562–565. https://doi.org/10.1111/j.1755-0998.2011.03108.x

Cubero-Leon, E., Peñalver, R., & Maquet, A. (2014). Review on metabolomics for food authentication. *Food Research International*, *60*, 95–107. https://doi.org/10.1016/j.foodres.2013.11.041

Cubero, O. F., Crespo, A., Fatehi, J., & Bridge, P. D. (1999). DNA extraction and PCR amplification method suitable for fresh, herbarium-stored, lichenized, and other fungi. *Plant Systematics and Evolution*, *216*(3–4), 243–249. https://doi.org/10.1007/BF01084401

Darriba, D., Taboada, G. L., Doallo, R., & Posada, D. (2012). jModelTest 2: more models, new heuristics and parallel computing. *Nature Methods*, *9*(8), 772–772. https://doi.org/10.1038/nmeth.2109

de Boer, H. J., Ichim, M. C., & Newmaster, S. G. (2015). DNA Barcoding and Pharmacovigilance of Herbal Medicines. *Drug Safety*, *38*(7), 611–620. https://doi.org/10.1007/s40264-015-0306-8

Fehrer, J., Slavíková-Bayerová, Š., & Orange, A. (2008). Large genetic divergence of new, morphologically similar species of sterile lichens from Europe (*Lepraria*, Stereocaulaceae, Ascomycota): Concordance of DNA sequence data with secondary metabolites. *Cladistics*, *24*(4), 443–458. https://doi.org/10.1111/j.1096-0031.2008.00216.x

Fernández-Moriano, C., Divakar, P. K., Crespo, A., & Gómez-Serranillos, M. P. (2015). Neuroprotective activity and cytotoxic potential of two Parmeliaceae lichens: Identification of active compounds. *Phytomedicine*, *22*(9), 847–855. https://doi.org/10.1016/j.phymed.2015.06.005

Galimberti, A., De Mattia, F., Losa, A., Bruni, I., Federici, S., Casiraghi, M., Martellos, S., Labra, M. (2013). DNA barcoding as a new tool for food traceability. *Food Research International*, *50*(1), 55–63. https://doi.org/10.1016/j.foodres.2012.09.036

Gardes, M., & Bruns, T. D. (1993). ITS primers with enhanced specificity for basidiomycetes, application to the identification of mycorrihiza and rusts. *Molecular Ecology*, *2*(May 2016), 113–118. https://doi.org/Doi 10.1111/J.1365-294x.1993.Tb00005.X

Gudjónsdóttir, G., & Ingólfsdóttir, K. (1997). Quantitative determination of protolichesterinic- and fumarprotocetraric acids in *Cetraria islandica* by high-performance liquid chromatography. *Journal of Chromatography A*, *757*(1–2), 303–306. https://doi.org/10.1016/S0021-9673(96)00670-X

Horhant, D., Lamer, a. C. L., Boustie, J., Uriac, P., & Gouault, N. (2007). Separation of a mixture of paraconic acids from *Cetraria islandica* (L.) Ach. employing a fluorous tag-catch and release strategy. *Tetrahedron Letters*, *48*(34), 6031–6033. https://doi.org/10.1016/j.tetlet.2007.06.077

Hossain, M. A. M., Ali, M. E., Abd Hamid, S. B., Asing, Mustafa, S., Mohd Desa, M. N., & Zaidul, I. S. M. (2016). Double Gene Targeting Multiplex Polymerase Chain Reaction-Restriction Fragment Length Polymorphism Assay Discriminates Beef, Buffalo, and Pork

Substitution in Frankfurter Products. *Journal of Agricultural and Food Chemistry*, *64*(32), 6343–6354. https://doi.org/10.1021/acs.jafc.6b02224

Hossain, M. A. M., Ali, M. E., Hamid, S. B. A., Asing, Mustafa, S., Desa, M. N. M., & Zaidul, I. S. M. (2017). Targeting double genes in multiplex PCR for discriminating bovine, buffalo and porcine materials in food chain. *Food Control*, *73*, 175–184. https://doi.org/https://doi.org/10.1016/j.foodcont.2016.08.008

Ingolfsdóttir, K. (2000). Bioactive compounds from Iceland Moss. In B. S. Paulsen (Ed.), *Bioactive Carbohydrate Polymers* (pp. 25–36). Springer Netherlands. https://doi.org/10.1007/978-94-015-9572-8_3

Katoh, K., & Standley, D. M. (2013). MAFFT multiple sequence alignment software version 7: Improvements in performance and usability. *Molecular Biology and Evolution*, *30*(4), 772–780. https://doi.org/10.1093/molbev/mst010

Kelly, L. J., Hollingsworth, P. M., Coppins, B. J., Ellis, C. J., Harrold, P., Tosh, J., & Yahr, R. (2011). DNA barcoding of lichenized fungi demonstrates high identification success in a floristic context. *New Phytologist*, *191*(1), 288–300. https://doi.org/10.1111/j.1469-8137.2011.03677.x

Kristinsson, H. (1969). Chemical and Morphological Variation in the Cetraria islandica Complex in Iceland. *The Bryologist*. https://doi.org/10.1639/0007-2745(1969)72[344:CAMVIT]2.0.CO;2

Leavitt, S. D., Esslinger, T. L., Hansen, E. S., Divakar, P. K., Crespo, A., Loomis, B. F., & Lumbsch, H. T. (2014). DNA barcoding of brown Parmeliae (Parmeliaceae) species: A molecular approach for accurate specimen identification, emphasizing species in Greenland. *Organisms Diversity and Evolution*, *14*(1), 11–20. https://doi.org/10.1007/s13127-013-0147-1

Liu, Y. J., Whelen, S., & Hall, B. D. (1999). Phylogenetic relationships among ascomycetes: evidence from an RNA polymerse II subunit. *Molecular Biology and Evolution*, *16*(12), 1799–1808. https://doi.org/10.1086/523946

Lumbsch, H. T. (1998). The use of metabolic data in lichenology at the species and subspecies levels. *Lichenologist*, *30*(4–5), 357–367.

Lutsak, T., Fernández-Mendoza, F., Nadyeina, O., Şenkardeşler, A., & Printzen, C. (2017). Testing the correlation between norstictic acid content and species evolution in the *Cetraria aculeata* group in Europe. *The Lichenologist*, *49*(1), 39–56. https://doi.org/10.1017/S0024282916000566

Mark, K., Cornejo, C., Keller, C., & Flück, D. (2016). Barcoding lichen-forming fungi using 454 pyrosequencing is challenged by artifactual and biological sequence variation. *Genome*, *704*(May), 1–56. https://doi.org/10.1139/gen-2015-0189

Messina, A., Callahan, D. L., Walsh, N. G., Hoebee, S. E., & Green, P. T. (2014). Testing the boundaries of closely related daisy taxa using metabolomic profiling. *Taxon*, *63*(2), 367–376. https://doi.org/10.12705/632.15

Meyer, C. P., & Paulay, G. (2005). DNA barcoding: Error rates based on comprehensive sampling. *PLoS Biology*, *3*(12), 1–10. https://doi.org/10.1371/journal.pbio.0030422

Mulzer, J., Salimi, N., & Hartl, H. (1993). First asymmetric synthesis of (+)- and (-)-Roccellaric acid and dihydroprotolichesterinic acid. *Tetrahedron: Asymmetry*, *4*(3), 457–471. https://doi.org/10.1016/S0957-4166(00)86089-9

Paradis, E., Claude, J., & Strimmer, K. (2004). APE: Analyses of phylogenetics and evolution in R language. *Bioinformatics*, *20*(2), 289–290. https://doi.org/10.1093/bioinformatics/btg412

Parrot, D., Jan, S., Baert, N., Guyot, S., & Tomasi, S. (2013). Comparative metabolite profiling and chemical study of *Ramalina siliquosa*

complex using LC-ESI-MS/MS approach. *Phytochemistry*, *89*, 114–124. https://doi.org/10.1016/j.phytochem.2013.02.002

Pino-Bodas, R., Martín, M. P., Burgaz, A. R., & Lumbsch, H. T. (2013). Species delimitation in *Cladonia* (Ascomycota): A challenge to the DNA barcoding philosophy. *Molecular Ecology Resources*, *13*(6), 1058–1068. https://doi.org/10.1111/1755-0998.12086

Raja, H. A., Baker, T. R., Little, J. G., & Oberlies, N. H. (2017). DNA barcoding for identification of consumer-relevant mushrooms: A partial solution for product certification? *Food Chemistry*, *214*, 383–392. https://doi.org/10.1016/j.foodchem.2016.07.052

Schoch, C. L., Seifert, K. a., Huhndorf, S., Robert, V., Spouge, J. L., Levesque, C. A., Chen, W., Fungal Barcoding Consortium. (2012). Nuclear ribosomal internal transcribed spacer (ITS) region as a universal DNA barcode marker for Fungi. *Proceedings of the National Academy of Sciences of the United States of America*, *109*(16), 1–6. https://doi.org/10.1073/pnas.1117018109

Staats, M., Arulandhu, A. J., Gravendeel, B., Holst-Jensen, A., Scholtens, I., Peelen, T., Prins, T.W., Kok, E. (2016). Advances in DNA metabarcoding for food and wildlife forensic species identification. *Analytical and Bioanalytical Chemistry*, 4615–4630. https://doi.org/10.1007/s00216-016-9595-8

Stamatakis, A. (2014). RAxML version 8: A tool for phylogenetic analysis and post-analysis of large phylogenies. *Bioinformatics*, *30*(9), 1312–1313. https://doi.org/10.1093/bioinformatics/btu033

Syers, J. K. (1969). Chelating ability of fumarprotocetraric acid and *Parmelia conspersa*. *Plant and Soil*, *31*(1), 205–208. https://doi.org/10.1007/BF01373043

Thell, A., & Moberg, R. (2011). *Nordic Lichen Flora. Volume 4. Parmeliaceae*. Museum of Evolution, Uppsala University.

Thell, A., Stenroos, S., & Myllys, L. (2000). A DNA study of the *Cetraria aculeata* and *C. islandica* groups. *Folia Cryptog. Estonica. Fasc.*, *36*, 95–106.

Větrovský, T., Kolařík, M., Žifčáková, L., Zelenka, T., & Baldrian, P. (2016). The rpb2 gene represents a viable alternative molecular marker for the analysis of environmental fungal communities. *Molecular Ecology Resources*, *16*(2), 388–401. https://doi.org/10.1111/1755-0998.12456

White, T. J., Bruns, T., Lee, S., & Taylor, J. W. (1990). Amplification and direct sequencing of fungal ribosomal RNA genes for phylogenetics. In M. A. Innis, D. H. Gelfand, J. J. Sninsky, & T. J. White (Eds.), *PCR Protocols: a Guide to Methods and Applications* (pp. 315–322). San Diego, USA: Academic Press INC.

Xu, M., Heidmarsson, S., Olafsdottir, E. S., Buonfiglio, R., Kogej, T., & Omarsdottir, S. (2016). Secondary metabolites from cetrarioid lichens: chemotaxonomy, biological activities and pharmaceutical potential. *Phytomedicine*, *23*(5), 441–459. https://doi.org/10.1016/j.phymed.2016.02.012

Xu, M., Heidmarsson, S., Thorsteinsdottir, M., Eiriksson, F. F., Omarsdottir, S., & Olafsdottir, E. S. (2017). DNA barcoding and LC-MS metabolite profiling of the lichen-forming genus Melanelia : Specimen identification and discrimination focusing on Icelandic taxa. *PLoS ONE*, *12*(5), e0178012. https://doi.org/10.1371/journal. pone.0178012

Figure captions

**Figure 1.** Morphological variation and similarity of Iceland Moss (*Cetraria islandica*) chemotypes and its sibling species *Cetraria ericetorum. C. islandica* shows considerable morphological variation, from wide (**a** and **c**) to narrow thallus (**b** and **d**). Two chemotypes were identified in *C. islandica* specimens using *p*-phenylendiamine (PD) spot testing/staining, including PD+ (red medullary color after staining; **a** and **b**) and PD- (no red medullary color after staining; **c** and **d**). The lichen *C. ericetorum* (**e**) is uniformly PD- and has narrow thallus. Scale: 1 cm.

**Figure 2.** Chemical structures of major lichen secondary metabolites detected in the *Cetraria islandica* species complex. Compounds include protocetraric acid **1**, succinprotocetraric acid **2**, fumarprotocetraric acid **3**, virensic acid **4**, nephrosterinic acid **5**, (+)-roccellaric acid **6**, (+)-protolichesterinic acid **7** and (+)-lichesterinic acid **8**. Minor compounds refer to Table S2.

**Figure 3.** MS chromatograms of the PD+ (**a**) and PD- (**b**) chemotypes of *Cetraria islandica* and PD- *C. ericetorum* (**c**) and thallus color reaction by PD staining of PD+ (**d**) and PD- (**e**) chemotypes of *Cetraria islandica* and PD- *C. ericetorum* (**f**).

Major secondary metabolites are labelled corresponding to structures **1**-**8** in Figure 2. Compounds **7A** and **7B** were tentatively identified as stereoisomers of (+)-protolichesterinic acid **7**, and **6A** a stereoisomer of (+)-roccellaric acid **6**. Scale = 0.5 mm.

**Figure 4.** PCA plot giving an overview of metabolite data and indicative grouping of species and chemotypes in the *Cetraria islandica* species complex. Three chemical groups include PD- chemotype (CI PD-), *C. islandica* PD+ chemotype (CI PD+) and *C. ericetorum* (CE). Authentic herbarium specimens were marked as dark green (CI PD+), dark red (CI PD-) and grey (CE).

**Figure 5.** Maximum likelihood (ML) trees of the *Cetraria islandica* species complex reconstructed using barcode markers. (**a**) ML tree reconstructed using the nrITS barcode, with *C. ericetorum* specimens marked in red; (**b**) ML tree using the RPB2 marker, where tree well-supported clades were identified: I, II and III. The PD+ chemotype is labelled with a red dot after each specimen. Bootstrap values > 70 are shown above branches in both trees.

**Figure 6.** Barcoding gap analysis of *Cetraria islandica* species complex for each marker. (**a**) Number of false positive and

644 false negative identifications along a threshold from 0.1% – 4%
645 DNA divergence; (**b**) Evaluation of inter- vs. intraspecific
646 divergence. The distances for each gene were calculated
647 according to the best model of evolution. Samples that are in
648 the top-left half of the plot have a greater minimum
649 interspecific than maximum intraspecific divergence and
650 exhibit a barcode gap.


b
c
d

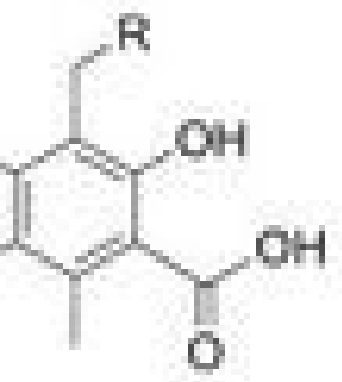


1

$H_2O_4$ 2

$H_2O_4$ 3

6

7

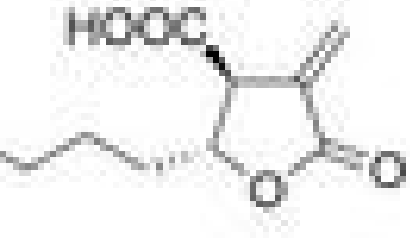


8

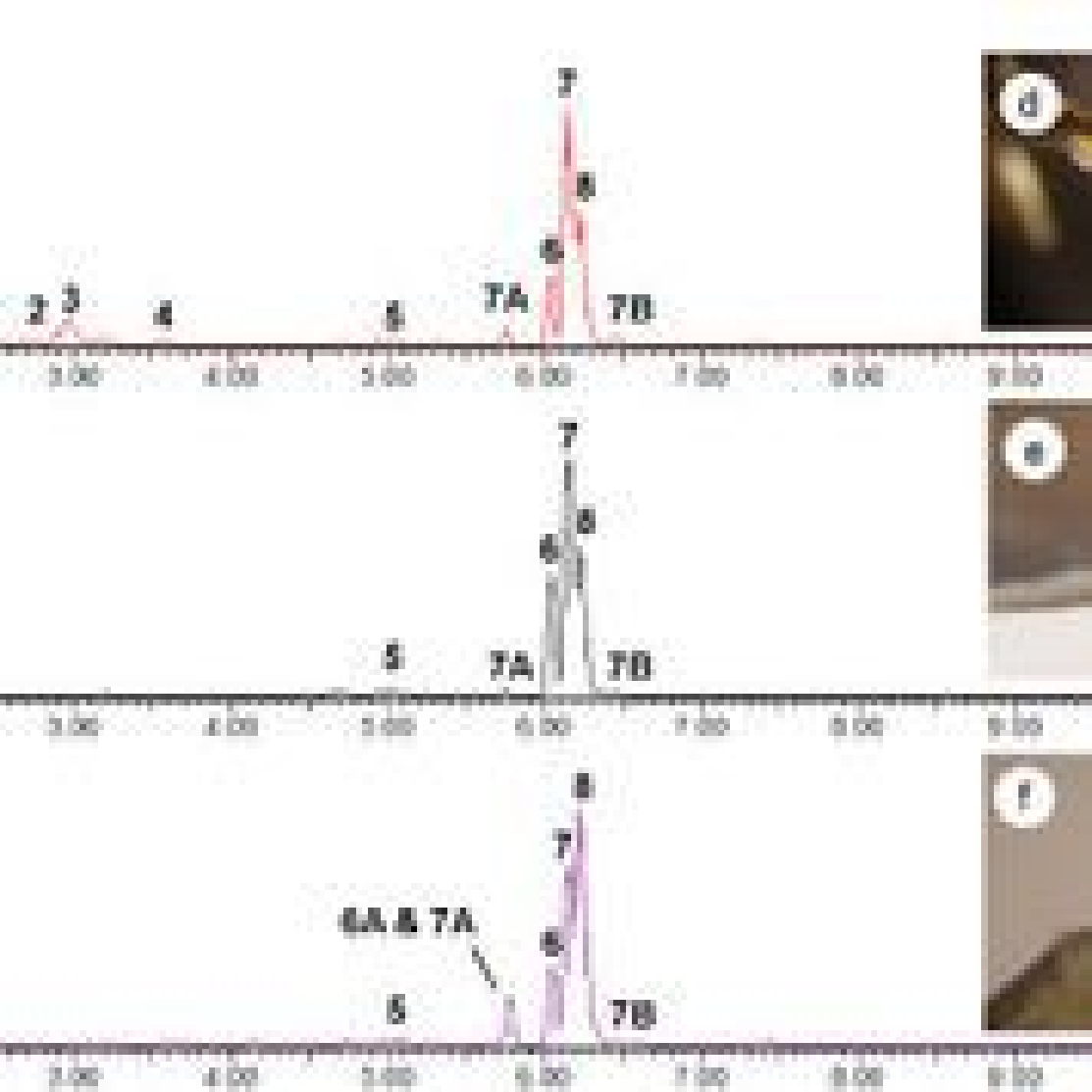
7
8
6
2
3
4
5
7A
7B
d
7
8
6
5
7A
7B
e
8
7
6A & 7A
6
5
7B
f

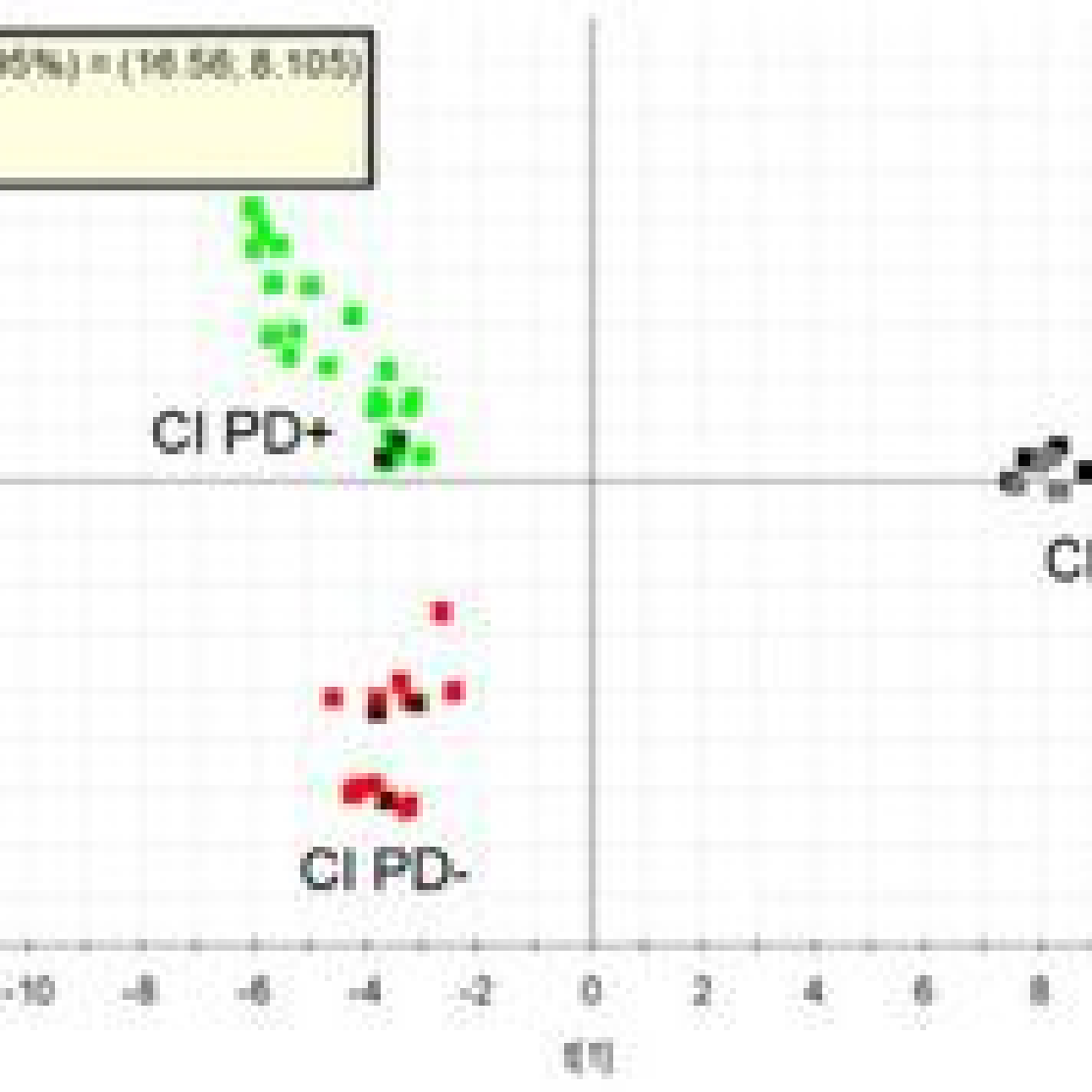
Cl PD+
Cl PD-
-10
-8
-6
-4
-2
0
2
4
6
8

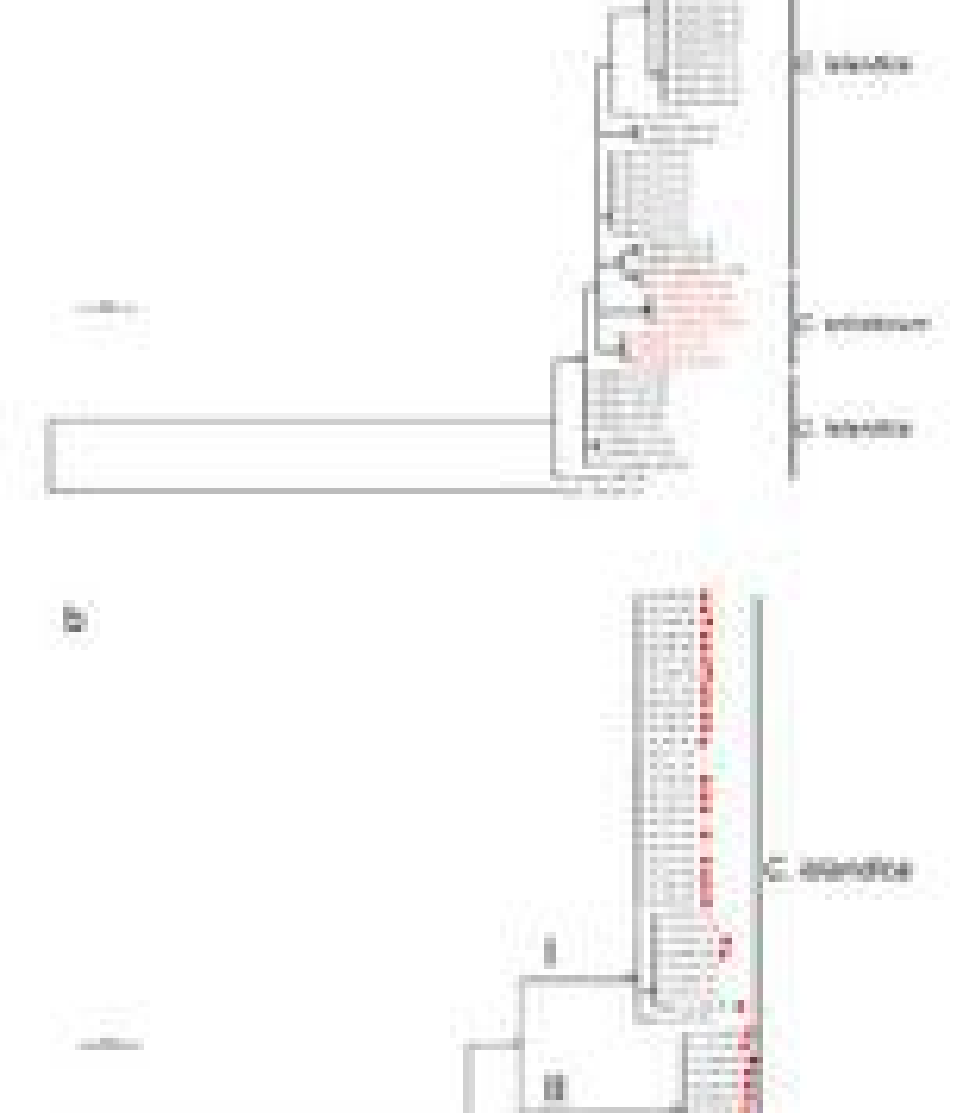
C. infantica
C. infantissima
C. infantica
b
C. asiatica
I
II

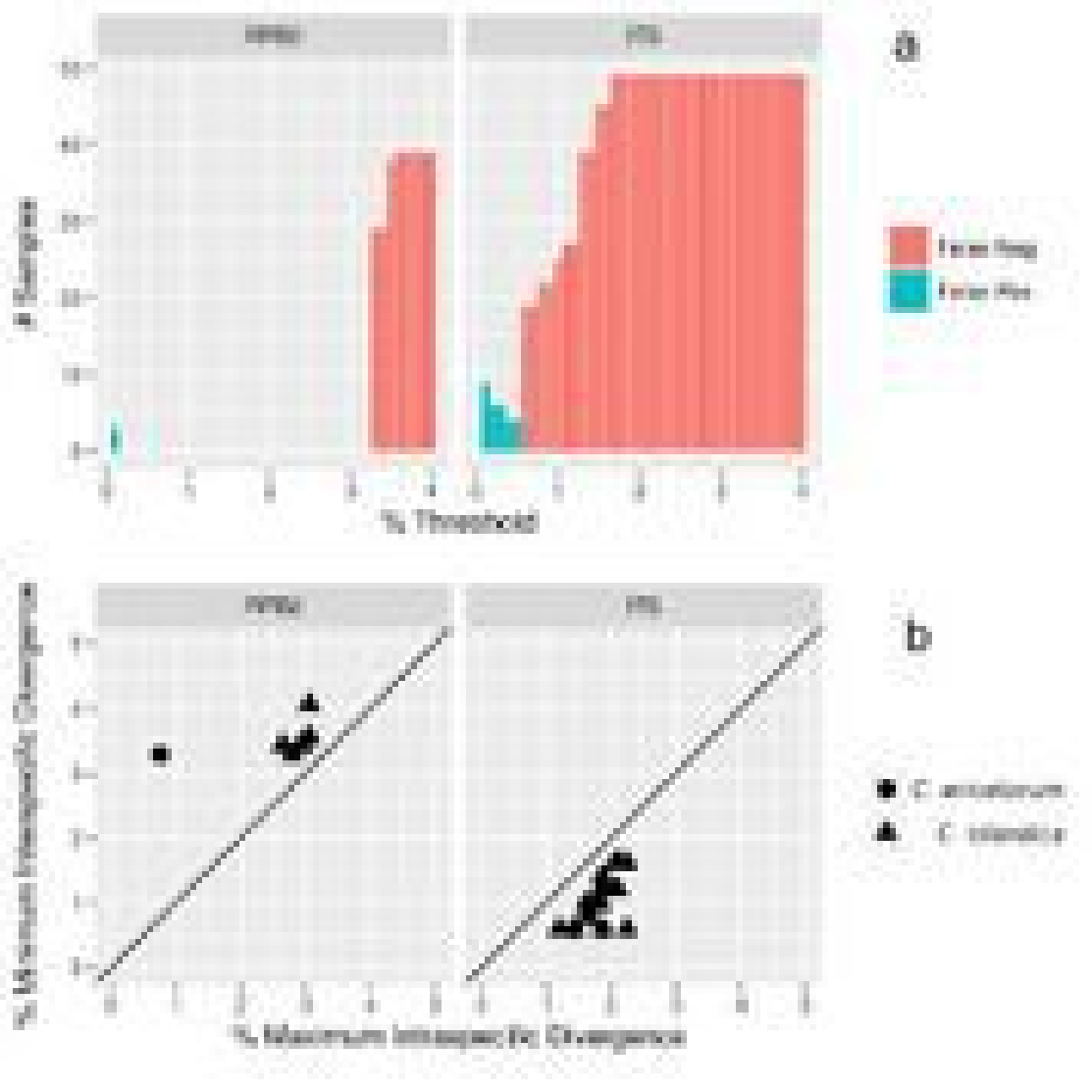
a
b
% Threshold

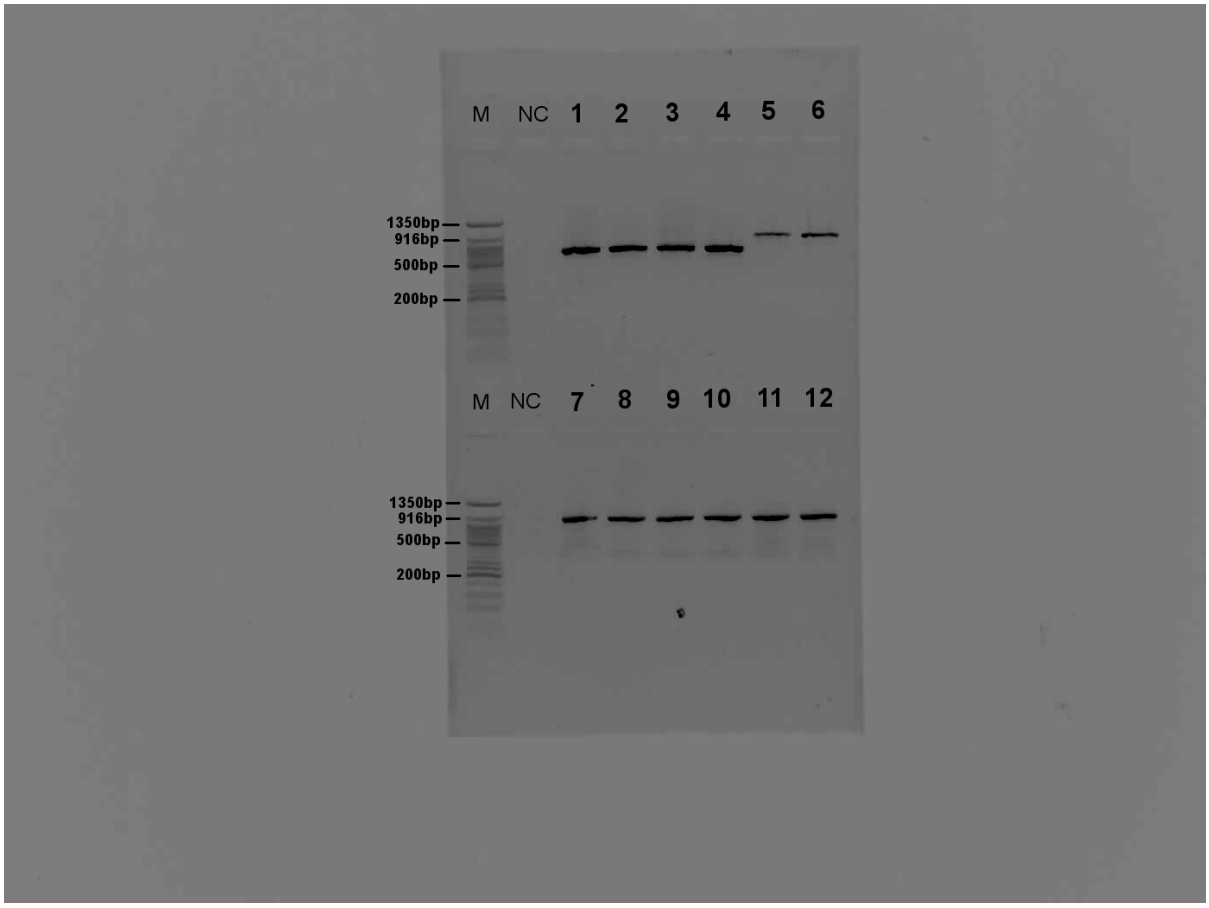


**Figure S1.** Agarose gel electrophoresis of PCR products from fungal nrITS and RPB2 loci. Lane 1-6: PCR products of fungal nrITS locus, ranging from 600 (intron-absent) to 900 bp (intron-present). Lane 7-12: PCR products of fungal RPB2 locus of ca. 900 bp. M: ladder. NC: negative control.

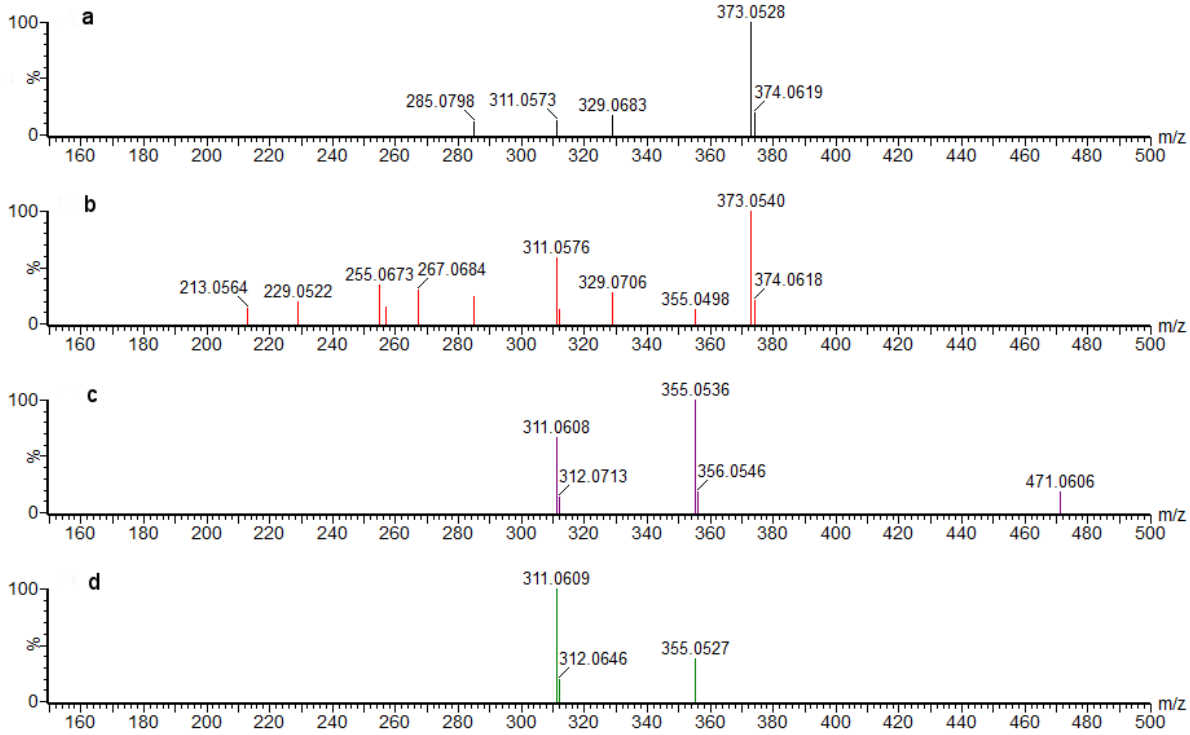


**Figure S2.** MS spectra of major depsidones in the PD+ *Cetraria islandica* chemotype. MS (**a**) and $MS^2$ (**b**) spectra for protocetraric acid **1**; MS (**c**) and $MS^2$ (**d**) spectra for fumarprotocetraric acid **3**.

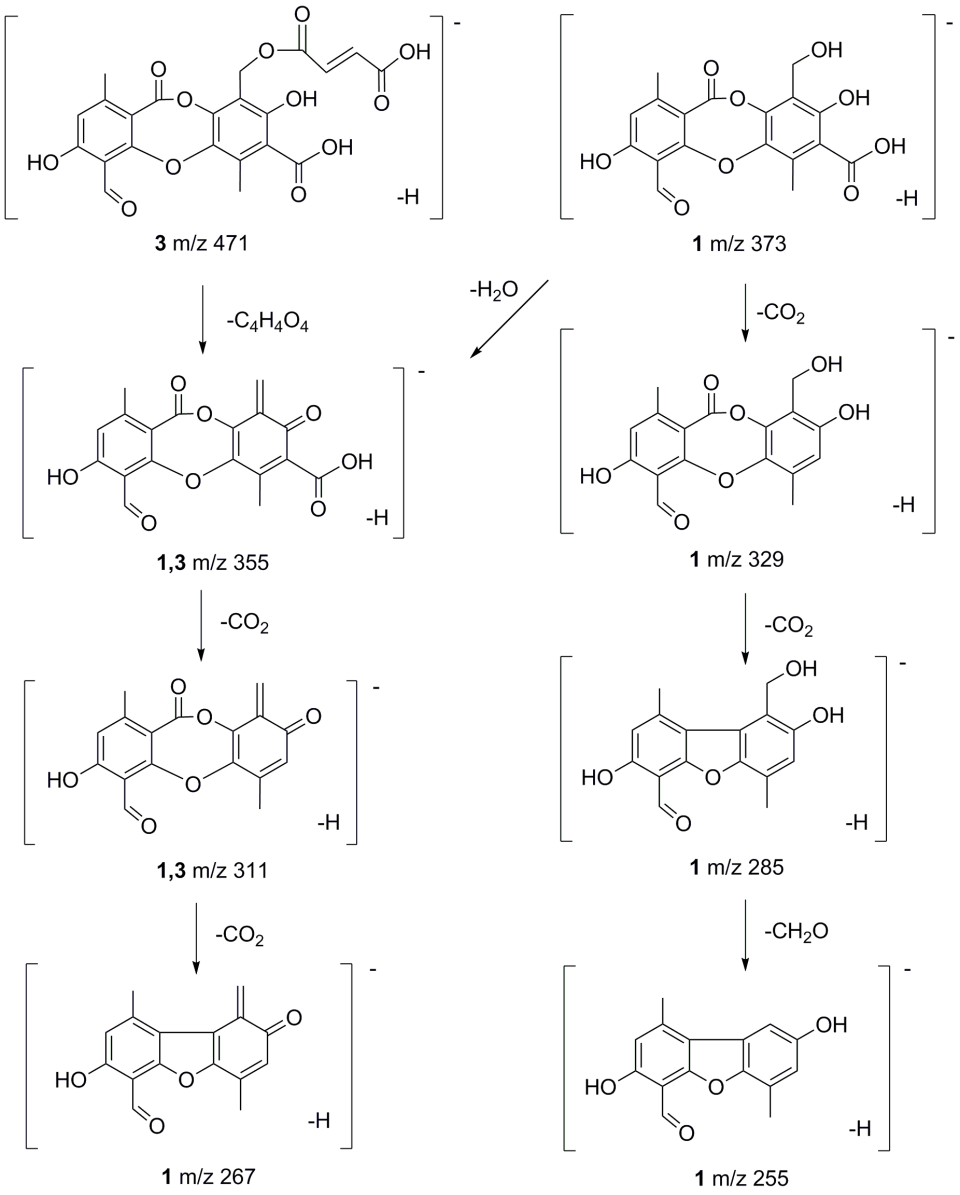


**Figure S3.** MS fragmentation patterns for major depsidones (protocetraric acid **1**; fumarprotocetraric acid **3**) in the PD+ *Cetraria islandica* chemotype.

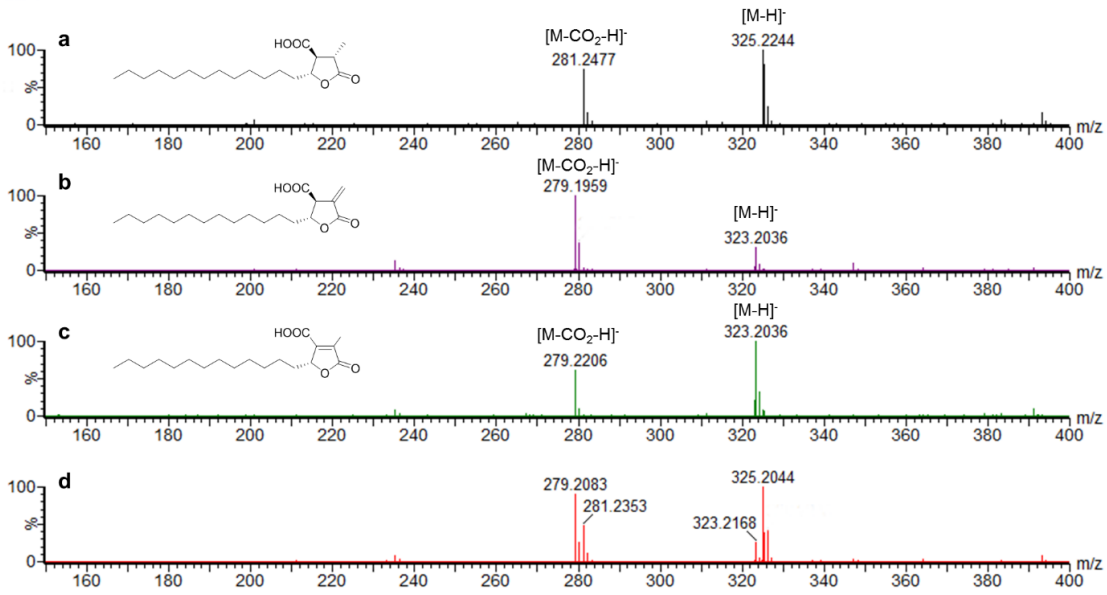


**Figure S4.** MS spectra for major paraconic acids in *Cetraria islandica* species complex. (**a**) MS spectrum of (+)-roccellaric acid **6**; (**b**) MS spectrum of (+)-protolichesterinic acid **7**; (**c**) MS spectrum of (+)-lichesterinic acid **8**. MS fragment ions of compounds **7** and **8** differed in the ratio of molecular ion $[M-H]^-$ to the decarboxylated molecular ion $[M-CO_2-H]^-$. The higher stability of lichesterinic acid molecular ion could be explained by hyperconjugation, where the electrons in the C-C bond between lactone ring and carboxylic group interacts with the unhybridized *p*-orbital in the adjacent ethylenic carbon; (**d**) MS spectrum of the peak eluting out at $t_R$ 5.87 min containing two compounds **6A** and **7A** in Fig 3. They are tentatively identified as a stereoisomer (compound **6A**; m/z 325.2 and 281.2) of **6** and a stereoisomer (compound **7A**; m/z 323.2 and 279.2) of **7**, respectively.

**Table S1.** Voucher specimens of *Cetraria islandica* species complex used in the current study, including country, collection date, voucher number, spot test results/chemotype, DNA isolate number and GenBank accession numbers.

| Country[a] | Collection date | Specimen voucher[b] | Spot test[c] | Collector | DNA Isolate | GenBank accession number | |
|---|---|---|---|---|---|---|---|
| | | | | | | RPB2 | nrITS |
| ***Cetraria islandica*** | | | | | | | |
| Iceland: IVe | 21-Aug-2012 | **LA31863** | PD+ | Starri Heidmarsson | CI1 | KY768945 | KY764967 |
| Iceland: IAu | 16-Aug-2012 | **LA31864** | PD+ | Starri Heidmarsson | CI4 | KY768946 | KY764968 |
| Iceland: INo | 21-Aug-2012 | LA31865 | PD+ | Starri Heidmarsson | CI6 | KY768947 | KY764969 |
| Iceland: IVe | 23-Aug-2012 | LA31866 | PD+ | Starri Heidmarsson | CI7 | KY768948 | KY764970 |
| Iceland: INo | 8-Jul-2013 | LA31867 | PD- | Starri Heidmarsson | CI11 | KY768949 | KY764971 |
| Iceland: IVe | 23-Jul-2013 | LA31868 | PD+ | Starri Heidmarsson | CI12 | KY768950 | KY764972 |
| Iceland: IVe | 25-Jul-2013 | LA31869 | PD+ | Starri Heidmarsson | CI13 | KY768951 | KY764973 |
| Iceland: IVe | 25-Jul-2013 | LA31870 | PD+ | Starri Heidmarsson | CI14 | KY768952 | KY764974 |
| Iceland: INo | 16-Aug-2012 | LA31871 | PD+ | Starri Heidmarsson | CI15 | KY768953 | KY764975 |
| Iceland: ISu | 12-Jul-2013 | LA31872 | PD+ | Starri Heidmarsson | CI16 | KY768954 | KY764976 |
| Iceland: IVe | 11-Jul-2013 | LA31873 | PD+ | Starri Heidmarsson | CI17 | KY768955 | KY764977 |
| Iceland: IVe | 11-Jul-2013 | LA31874 | PD+ | Starri Heidmarsson | CI18 | KY768956 | KY764978 |
| Iceland: IVe | 23-Jul-2013 | LA31875 | PD+ | Starri Heidmarsson | CI19 | KY768957 | KY764979 |
| Iceland: IVe | 9-Aug-2013 | LA31876 | PD+ | Starri Heidmarsson | CI25 | KY768958 | KY764980 |
| Iceland: IVe | 23-Jul-2013 | LA31877 | PD+ | Starri Heidmarsson | CI26 | KY768959 | KY764981 |
| Iceland: IVe | 8-Jul-2013 | LA31878 | PD+ | Starri Heidmarsson | CI27 | KY768960 | KY764982 |
| Iceland: IVe | 8-Jul-2013 | LA31879 | PD+ | Starri Heidmarsson | CI28 | KY768961 | KY764983 |
| Iceland: IVe | 11-Jul-2013 | LA31880 | PD+ | Starri Heidmarsson | CI29 | KY768962 | KY764984 |
| Iceland: IVe | 8-Jul-2013 | LA31881 | PD+ | Starri Heidmarsson | CI30 | KY768963 | KY764985 |
| Iceland: IVe | 21-Aug-2013 | LA31882 | PD+ | Starri Heidmarsson | CI31 | KY768964 | KY764986 |
| Iceland: IVe | 8-Jul-2013 | LA31883 | PD+ | Starri Heidmarsson | CI32 | KY768965 | KY764987 |
| Iceland: INo | 24-Jul-2012 | LA31884 | PD- | Starri Heidmarsson | CI57a | KY768966 | KY764988 |
| Iceland: INo | 24-Jul-2012 | LA31885 | PD- | Starri Heidmarsson | CI57b | KY768967 | KY764989 |
| Iceland: INv | 30-Aug-2013 | LA31886 | PD+ | Starri Heidmarsson | CI58 | KY768968 | KY764990 |
| Iceland: IAu | 15-Aug-2012 | LA31887 | PD+ | Starri Heidmarsson | CI59 | KY768969 | KY764991 |

| | | | | | | | |
|---|---|---|---|---|---|---|---|
| Iceland: INv | 22-Aug-2013 | LA31888 | PD- | Starri Heidmarsson | CI60 | KY768970 | KY764992 |
| Iceland: INv | 26-Aug-2013 | LA31889 | PD- | Starri Heidmarsson | CI61 | KY768971 | KY764993 |
| Iceland: INo | 14-Aug-2012 | LA31890 | PD+ | Starri Heidmarsson | CI62 | KY768972 | KY764994 |
| Iceland: IVe | 15-Aug-2012 | LA31928 | PD+ | Starri Heidmarsson | CI63 | KY768973 | KY764995 |
| Iceland: INo | 21-Aug-2012 | LA31891 | PD+ | Starri Heidmarsson | CI64 | KY768974 | KY764996 |
| Iceland: INo | 28-Jun-2012 | LA31929 | PD- | Starri Heidmarsson | CI65 | KY768975 | KY764997 |
| Iceland: IVe | 12-Jul-2013 | LA31892 | PD+ | Starri Heidmarsson | CI66 | KY768976 | KY764998 |
| Iceland: INv | 22-Aug-2013 | LA31893 | PD- | Starri Heidmarsson | CI67 | KY768977 | KY764999 |
| Iceland: INo | 24-Jun-2012 | LA31894 | PD+ | Starri Heidmarsson | CI68 | KY768978 | KY765000 |
| Iceland: INo | 2012 | LA31895 | PD- | Starri Heidmarsson | CI69 | KY768979 | KY765001 |
| Iceland: INo | 2012 | LA31896 | PD- | Starri Heidmarsson | CI70 | KY768980 | KY765002 |
| Iceland: INo | 8-Aug-2012 | LA31897 | PD+ | Starri Heidmarsson | CI77 | KY768981 | KY765003 |
| Iceland: INo | 28-Jun-2012 | LA31898 | PD+ | Starri Heidmarsson | CI78a | KY768982 | KY765004 |
| Iceland: INo | 28-Jun-2012 | LA31899 | PD+ | Starri Heidmarsson | CI78b | KY768983 | KY765005 |
| Iceland: INo | 23-Aug-2012 | LA31927 | PD- | Starri Heidmarsson | CI87a | KY768984 | KY765006 |
| Iceland: INo | 11-Jul-2002 | **LA30017** | PD- | Hordur Kristinsson | CI115 | KY768985 | KY765007 |
| Iceland: INo | 14-Aug-2012 | LA31900 | PD- | Starri Heidmarsson | CI117a | KY768986 | KY765008 |
| Iceland: INo | 10-Aug-2006 | **LA31128** | PD- | Hordur Kristinsson | CI113 | - | - |
| Iceland: INo | 10-Jul-1998 | **LA17549** | PD- | Hordur Kristinsson | CI36 | - | - |
| Iceland: INo | 5-Jul-1998 | **LA17221** | PD- | Hordur Kristinsson | CI37 | - | - |
| ***Cetraria ericetorum*** | | | | | | | |
| Iceland:IAu | 10-Aug-1997 | LA18976 | PD- | Hordur Kristinsson | CE1 | - | KY765009 |
| Finland: Sodankylä | 21-Aug-2003 | **NO2530** | PD- | Beata Krewicka | CE6 | KY768987 | KY765010 |
| Sweden: Uppsala | 20-May-2002 | **NO23002** | PD- | Leif Tibell | CE8 | KY768988 | KY765011 |
| Sweden: Uppsala | 18-Oct-2015 | **NO5626** | PD- | Stefan Ekman | CE11 | KY768989 | KY765012 |
| Iceland: IAu | 13-Jul-2014 | LA20746 | PD- | Hordur Kristinsson | CE13 | KY768990 | KY765013 |
| Iceland: INo | 29-Aug-2016 | LA31901 | PD- | Hordur Kristinsson | CE15 | KY768991 | KY765014 |
| Iceland: INo | 1-Sep-2010 | LA31538 | PD- | Hordur Kristinsson | CE16 | KY768992 | KY765015 |
| Iceland: IAu | 9-Aug-1997 | LA27354 | PD- | Hordur Kristinsson | CE2 | - | - |

| | | | | | | | |
|---|---|---|---|---|---|---|---|
| Sweden: Gävleborg | 15-Jun-1997 | **NO501** | PD- | Ake Agren | CE3 | - | - |
| Russian: Komi | 6-Jul-2000 | **L135019** | PD- | - | CE4 | - | - |
| Canada: Quebec | 2-Jul-1999 | **NO5021** | PD- | Jan-Eric Mattsson | CE5 | - | - |
| Poland: Silesia | 19-Jul-1998 | **KO2101** | PD- | - | CE7 | - | - |
| Russia: Komi | 2-Jul-1997 | **NO7971** | PD- | Björn Larsson | CE9 | - | - |
| Iceland: INo | 31-Jul-1996 | **NO720** | PD- | Starri Heidmarsson | CE10 | - | - |
| Iceland: INo | 18-Aug-1998 | LA20809 | PD- | Hordur Kristinsson | CE12 | - | - |
| Iceland: INo | 7-Jun-1998 | LA18310 | PD- | Hordur Kristinsson | CE14 | - | - |
| Iceland: INo | 19-Aug-1998 | LA29284 | PD- | Hordur Kristinsson | CE17 | - | - |
| Iceland: INo | 10-Aug-1997 | LA18982 | PD- | Hordur Kristinsson | CE18 | - | - |

[a] INo, INv, IVe, IMi, IAu and ISu refer to corresponding area in Icelandic map below;

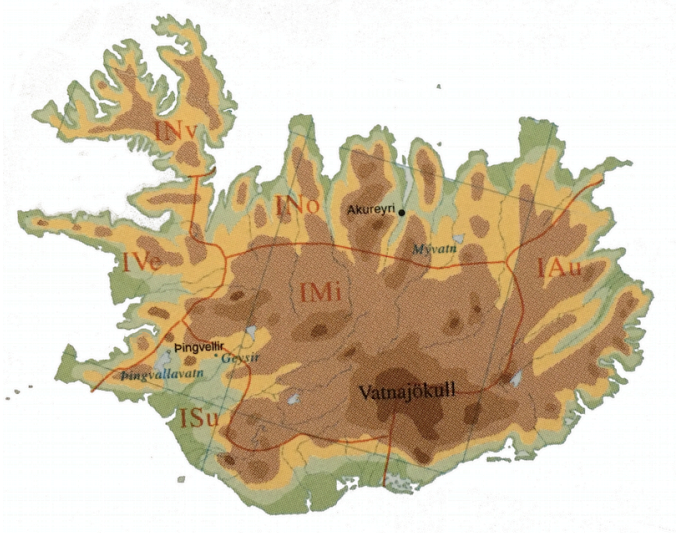


[b] Authentic herbarium specimens are marked in boldface;
[c] Spot testing/chemotype identification results are reported as PD+ (medullary red color after *p*-phenylendiamine staining) and PD- (no red color after *p*-phenylendiamine staining).

**Table S2.** Chromatographic and MS data of metabolites tentatively identified from acetone extracts of taxa in the *Cetraria islandica* species complex.

| $t_R$ (min)[a] | $[M-H]^-$ (m/z)[b] | Product ions (m/z)[c] | Mass error (ppm)[d] | Molecular formula | Compound[e] | Lichen[f] |
|---|---|---|---|---|---|---|
| 2.48 | 373.0540 | 355.0498, 329.0706, 311.0576, 285.0798 | -5.4 | $C_{18}H_{14}O_9$ | Protocetraric acid **1** | CI (PD+) |
| 2.55 | 385.0650 | 341.0783, **329.2408** | - | - | Unidentified | CE |
| 2.67 | 487.0986 | 373.0665, **355.0501**, 311.0594 | - | - | Unidentified | CI (PD+) |
| 2.75 | 473.0806 | **355.0451**, 311. 0550 | -0.8 | $C_{22}H_{18}O_{12}$ | Succinprotocetraric acid **2** | CI (PD+) |
| 2.88 | 517.1052 | 401.0900, 369.0647, 325.0730 | 6.7 | - | Unidentified | CI (PD+) |
| 2.96 | 471.0536 | **355.0467**, 311.0581 | -1.4 | $C_{22}H_{16}O_{12}$ | Fumarprotocetraric acid **3** | CI (PD+) |
| 3.07 | 489.3547 | 355.0500, **343.0474**, 311.0598, 299,0618 | - | - | Unidentified | CI (PD+) |
| 3.17 | 387.0728 | 355.0474, 343.0864, 311.0580, 299.0962 | 3.1 | $C_{19}H_{16}O_9$ | Unidentified | CI (PD+) |
| 3.21 | 293.1744 | 236.1066, 221.1552 | -3.1 | $C_{17}H_{26}O_4$ | Unidentified | CI, CE |
| 3.34 | 431.3405 | 355.0503, 309.1720 | 7.4 | $C_{24}H_{48}O_6$ | Unidentified | CI (PD+) |
| 3.57 | 357.0607 | 313.0723, 269.0848 | -0.8 | $C_{18}H_{14}O_8$ | Virensic acid **4** | CI (PD+) |
| 4.17 | 295.2257 | 277.2194, 171.1052 | -5.4 | $C_{18}H_{32}O_3$ | Unidentified | CE |
| 4.71 | - | 443.3083, **279.2310**, 250.1470 | -5.0 | - | Unidentified | CI, CE |
| 4.94 | - | 297.2133, **279.2383**, 264.1647, 253.2214 | - | - | Unidentified | CI, CE |
| 5.03 | 279.2364 | **251.2069** | - | - | Unidentified | CI, CE |
| 5.09 | 295.1935 | 251.2062 | 8.8 | $C_{17}H_{28}O_4$ | Nephrosterinic acid **5** | CI, CE |
| 5.44 | - | 311.2299, **281.2556** | - | - | Unidentified | CI, CE |
| 5.77 | 323.2168 | **279.2314** | -3.6 | $C_{19}H_{32}O_4$ | A stereoisomer of (+)-Protolichesterinic acid **7A** | CI, CE |
| 5.77 | 325.2370 | 281.2527 | -2.8 | $C_{19}H_{34}O_4$ | A stereoisomer of (+)-Roccellaric acid **6A** | CE |
| 6.05 | 325.2405 | 281.2511 | 8.0 | $C_{19}H_{34}O_4$ | (+)-Roccellaric acid **6** | CI, CE |
| 6.17 | 323.2234 | **279.2322** | -0.7 | $C_{19}H_{32}O_4$ | (+)-Protolichesterinic acid **7** | CI, CE |
| 6.23 | 323.2224 | 279.2372 | 0.6 | $C_{19}H_{32}O_4$ | Lichesterinic acid **8** | CI, CE |
| 6.46 | 323.2218 | **279.2336** | 4.5 | $C_{19}H_{32}O_4$ | A stereoisomer of (+)-Protolichesterinic acid **7B** | CI, CE |

[a] $t_R$ means retention time;
[b] $[M-H]^-$ stands for deprotonated molecular ion;
[c] The product ion is marked in bold when it is the base peak in the MS spectrum;
[d] The mass error of the base peak is provided;
[e] Major compounds **1-8** are labelled corresponding to structures in Figure 2;
[f] The presence of lichen compounds in lichen taxa. CI (PD+): the PD+ chemotype of *Cetraria islandica*; CI: both PD+ and PD- chemotypes of *C. islandica*; CE: *C. ericetorum*.